Artificial metalloenzymes based on biotin-avidin technology for the enantioselective reduction of ketones by transfer hydrogenation

Christophe Letondor*, Nicolas Humbert*, and Thomas R. Ward†

Institute of Chemistry, University of Neuchâtel, Avenue Bellevaux 51, CP 2, CH-2007 Neuchâtel, Switzerland

Edited by Jack Halpern, University of Chicago, Chicago, IL, and approved February 9, 2005 (received for review December 23, 2004)

Most physiological and biotechnological processes rely on molecular recognition between chiral (handed) molecules. Manmade homogeneous catalysts and enzymes offer complementary means for producing enantiopure (single-handed) compounds. As the subtle details that govern chiral discrimination are difficult to predict, improving the performance of such catalysts often relies on trial-and-error procedures. Homogeneous catalysts are optimized by chemical modification of the chiral environment around the metal center. Enzymes can be improved by modification of gene encoding the protein. Incorporation of a biotinylated organometallic catalyst into a host protein (avidin or streptavidin) affords versatile artificial metalloenzymes for the reduction of ketones by transfer hydrogenation. The boric acid·formate mixture was identified as a hydrogen source compatible with these artificial metalloenzymes. A combined chemo-genetic procedure allows us to optimize the activity and selectivity of these hybrid catalysts: up to 94% (*R*) enantiomeric excess for the reduction of *p*-methylacetophenone. These artificial metalloenzymes display features reminiscent of both homogeneous catalysts and enzymes.

second coordination sphere | asymmetric catalysis | chemzymes

The asymmetric reduction of C═O and C═N bonds is one of the most fundamental transformations in organic chemistry (1–3). Although enzymatic and organometallic catalysis have evolved along very different paths, both methodologies can achieve high levels of enantioselection for this transformation.

Oxidoreductases such as alcohol dehydrogenases can perform this task very efficiently and selectively (4–7). To achieve this, however, these enzymes rely on precious cofactors NAD(P)H, which need to be regenerated (8). Alternatively, whole cells can be used. These contain multiple dehydrogenases, all of the necessary cofactors, and the metabolic pathways for their regeneration (5).

Asymmetric transfer hydrogenation (Meerwein-Ponndorf-Verley reduction) based on d^6 piano-stool complexes has proven to be versatile for the asymmetric reduction of ketones and imines (2, 9, 10). Regeneration of the organometallic hydride is achieved by a β-H abstraction between the catalyst precursor and a sacrificial hydrogen donor (isopropanol or formate). These catalysts nicely complement other organometallic systems that rely on dihydrogen (3).

It is interesting to note that theoretical studies suggest that the transfer hydrogenation catalyzed by d^6 piano-stool complexes proceeds without coordination of the substrate to the metal, as illustrated in transition-state structure **1** (11–14) (Fig. 1). The chiral recognition pattern for this organometallic transformation is thus reminiscent of enzymatic catalysis. Indeed, the second coordination sphere provided by a protein is optimized to steer the enantiodiscrimination step without necessarily requiring covalent (or dative) binding of the substrate to the enzyme.

In recent years, chemo-enzymatic catalysis has attracted increasing attention. In such systems, an enzyme is combined with an organometallic catalyst to afford versatile hybrid catalysts. In this context, the propensity of d^6 piano-stool metal complexes to undergo β-H abstraction in the presence of an alcohol or formate has been exploited in combination with enzymes to yield chemoenzymatic systems (15–20). For example, combining a lipase (which acylates exclusively one enantiomer of a secondary alcohol) with a $[\eta^5\text{-}(Ph_4C_5O^-)Ru^+(CO)_2]$ moiety (which racemizes the alcohol by β-H abstraction followed by an insertion) allows the dynamic kinetic resolution of secondary alcohols by acylation (15, 20). Another elegant hybrid catalyst example relies on the β-H abstraction propensity of $[\eta^5\text{-}(Me_5C_5)Rh(bpy)(H_2O)]^{2+}$ toward formate to regenerate the precious flavin cofactor of styrene monooxygenase and to produce (*S*)-styrene oxide from styrene in nearly enantiopure form [enantiomeric excess (ee) >99%] (19).

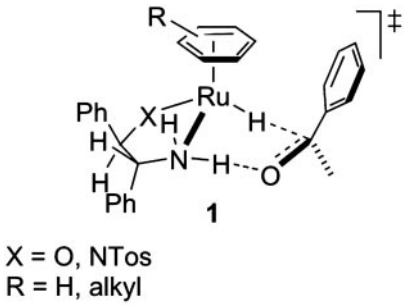

Fig. 1. Transition-state structure **1**.

These two examples of chemo-enzymatic catalysis demonstrate that the typical β-H abstraction–insertion reactivity of d^6 piano-stool complexes is maintained despite the abundance of donor functionalities present on the surface of an enzyme. With the aim of creating artificial transfer hydrogenases for the enantioselective reduction of ketones, we set out to anchor a d^6 piano-stool complex within a host protein. We reasoned that, as the substrate does not bind to the metal center during transfer hydrogenation (see **1**, Fig. 1), a well defined second coordination sphere provided by the host protein around a piano-stool complex offers an attractive mean for optimizing the selectivity of transfer hydrogenation catalysts. The general concept is outlined in Scheme 1.

With the aim of creating artificial metalloenzymes, both covalent and noncovalent anchoring strategies of organometallic species with a well defined first coordination sphere are currently being pursued by various groups (21–25). Inspired by the work of Wilson and Whitesides (26), we have recently exploited biotin-avidin technology to ensure the localization of a [Rh(diphosphine)]$^+$-moiety in a chiral environment provided by the (strept)avidin, (strept)avidin refers to either avidin or strepta-

This paper was submitted directly (Track II) to the PNAS office.

Abbreviation: ee, enantiomeric excess.

*C.L. and N.H. contributed equally to this work.

†To whom correspondence should be addressed. E-mail: thomas.ward@unine.ch.

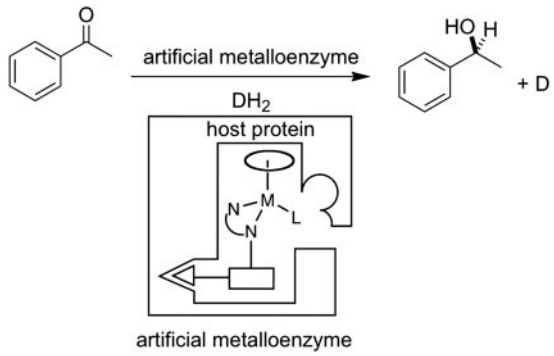

Scheme 1. Artificial metalloenzymes for enantioselective transfer hydrogenation reactions. The host protein displays high affinity for the anchor (triangle); introduction of a spacer (rectangle) and variation of the d^6 piano-stool moiety allows us to chemically optimize the enantioselectivity. Site-directed mutagenesis allows for a genetic optimization of the host protein.

vidin (26–30). Herein, we present our efforts to extend this methodology to the transfer hydrogenation of ketones by using biotinylated d^6 piano-stool complexes in conjunction with (strept)avidin.

Methods

(Strept)avidin was produced, purified, and quantified according to ref. 28. All experiments were carried out by using standard Schlenk techniques, with thoroughly degassed solutions (nitrogen-flushed).

Preparation of [η^6-(arene)Ru(Biot–*q*–L)Cl]. The ruthenium dimer [η^6-(arene)$RuCl_2]_2$ (arene = benzene, *p*-cymene; *q* = *ortho*, *meta*, *para*) (38.8 μmol, 1.00 eq.), the biotinylated ligand **Biot–*q*–LH** (37.8 mg, 85.5 μmol, 2.20 eq.), and NEt_3 (12.5 μl, 90 μmol, 2.25 eq.) were dissolved in isopropanol (1.5 ml) and heated at 80°C for 2 h. The solvent was removed *in vacuo* to afford a red-brown powder that was stored under nitrogen until use. For catalysis purposes, the crude catalyst precursor [η^6-(arene)Ru(**Biot–*q*–L**)Cl] was dissolved in degassed dimethylformamide to a final stock solution concentration of [Ru] = 0.0395 M. This stock solution can be stored for several days without any noticeable loss in activity or selectivity.

Boric Acid·Formate Mixed Buffer. Boric acid (1.05 g, 17 mmol) and sodium formate (1.36 g, 20 mmol) were dissolved in water (20 ml). The pH was adjusted to 6.25 with NaOH pellets. The final stock-solution concentration was $B(OH)_3$ = 0.85 M, HCO_2Na = 1 M.

Catalysis Experiments. (Strept)avidin was dissolved in water [100 μM tetrameric concentration (31)] and thoroughly degassed. The host protein (450 μl, 0.045 μmol, 1.4 eq. active sites vs. ruthenium) was mixed in a test tube (7 ml capacity) with the precursor complex [η^6-(arene)Ru(**Biot–*q*–L**)Cl] (3.3 μl of the dimethylformamide stock solution, 0.13 μmol ruthenium) and stirred at room temperature for 10 min. The boric acid·formate mixed buffer (550 μl of the stock solution, 42 eq. formate vs. substrate **2 a-c**), and, if required, the Mops buffer (200 μl of 1 M stock solution in water, pH 6.25, as well as an additional 50 μl of the boric acid·formate stock solution) were added and stirred for 5 min. Finally, substrate **2 a-c** (13 μl of a 1 M stock solution in dimethylformamide, 13 μmol, 100 eq. vs. ruthenium) was added. The test tube was placed in a magnetically stirred 24 multireactor (Greenhouse Parallel Synthesizer from Radleys, Brinkmann), purged four times with nitrogen, and heated at 45–55°C for 40–64 h. After completion, the reaction mixture was extracted four times with Et_2O (4 × 1 ml) and dried over Na_2SO_4. Subsequent continuous extraction of the resulting aqueous phase reveals no trace of substrate **2 a-c** or product **3 a-c**. The organic solution was filtered through a short silica plug that was thoroughly washed with Et_2O, concentrated, and subjected to HPLC analysis using a Chiralcel OB-H column (Daicel Chemical Industries, Tokyo) with hexane/isopropanol at 97:3 at 0.7 ml/min. Identical results were obtained for the best ees with samples that were not subjected to filtration through a silica plug.

For 1-phenylethanol **3a**, t_S = 18.18 min and t_R = 26.45 min (UV detection at 215 nm, absolute configuration determined with a commercial enantiopure sample).

For 1-(*p*-bromophenyl)ethanol **3b**, t_S = 17.33 min and t_R = 19.44 min [UV detection at 225 nm, absolute configuration (32)].

For 1-(*p*-methyphenyl)ethanol **3c**, t_S = 19.14 min and t_R = 22.16 min [UV detection at 215 nm, absolute configuration (33)].

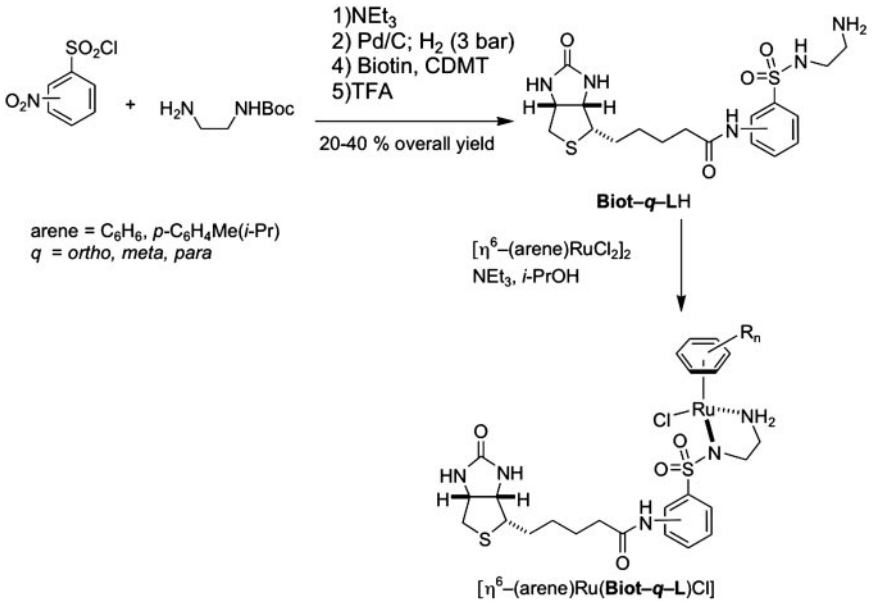

Scheme 2. Biotinylated ligand synthesis and *in situ* catalyst precursor generation. CDMT, 2-chloro-4,6-dimethoxy-1,3,5-triazine; TFA, trifluoracetic acid.

Results and Discussion

The most successful ligands for enantioselective transfer hydrogenation with d^6 piano-stool complexes in organic solvents are often amino alcohols, amino-sulfonamides, and diimine ligands (2, 9, 10, 34). In aqueous solvents, the most promising systems are based on water-soluble or polymer-supported amino-sulfonamide scaffolds derived from Noyori's system (35–40). In the same spirit, we synthesized a series of achiral aminosulfonamide ligands **Biot–*q*–L**H (Scheme 2) and set out to test their potential in combination with two $[\eta^6\text{-(arene)Ru}]^{2+}$ moieties by using (strept)avidin as host proteins.

The catalyst precursors $[\eta^6\text{-(arene)Ru(}$**Biot–*q*–L**$\text{)Cl}]$ were prepared *in situ* with isopropanol and triethylamine. Such complexes are chiral at ruthenium. The absence of a CD signal in their absorption band strongly suggests that these complexes are formed as a 1:1 mixture of epimers at ruthenium. As a consequence, in the absence of (strept)avidin, all catalysts (1 mol% vs. acetophenone **2a**) produce quantitatively (*rac*)-phenylethanol **3a** at 45°C within 40 h of using either isopropanol, the triethylamine·formic acid azeotropic mixture, or 1.5 M sodium formate as the hydrogen source. These experiments demonstrate that the catalyst precursors are indeed active, but unselective, transfer hydrogenation catalysts.

Under similar reaction conditions but in the presence of (strept)avidin {1 mol% $[\eta^6\text{-(cymene)Ru(}$**Biot–*p*–L**$\text{)Cl}]$, 0.34 mol% tetrameric streptavidin, Scheme 3}, we observed the slow appearance of a white precipitate. Nondenaturing gel electrophoresis (41, 42) of the turbid mixture reveals the presence of monomeric (strept)avidin, suggesting that these reducing agents denature (strept)avidin. Decreasing the formate concentration to 0.5 M (42 eq. vs. acetophenone) allows us to totally suppress the denaturation of the host protein, thus ensuring that the chiral environment provided by the host protein remains unaltered throughout catalysis [conversion 51%, ee 28% (*R*), Table 1, entry 1].

With the aim of stabilizing the pH during catalysis (43), various acids were screened in combination with 0.5 M sodium formate. These experiments revealed that the mixed buffer $HCO_2Na{\cdot}B(OH)_3$ ($pH_{initial}$ 6.25, pH_{final} <7.5 with boric acid, pH_{final} >8.5 without boric acid) has a beneficial effect on the ee [conversion 55%, ee 57% (*R*), Table 1, entry 2].

Having identified a reducing source compatible with the artificial metalloenzyme, we tested various biotinylated catalyst precursors $[\eta^6\text{-(arene)Ru(}$**Biot–*q*–L**$\text{)Cl}]$ in conjunction with WT (strept)avidin (WT-Avi and WT-Sav respectively; Table 1). These experiments reveal the following trends:

(*i*) The *para*-anchored ligand **Biot–*p*–L** outperforms both the *ortho*- and the *meta*-diastereomers **Biot–*o*–L** and **Biot–*m*–L** in terms of activity and selectivity (Table 1, compare entries 2, 4, and 5).

(*ii*) Streptavidin is a better host protein than avidin (Table 1, compare entries 2 and 3 and 6 and 7).

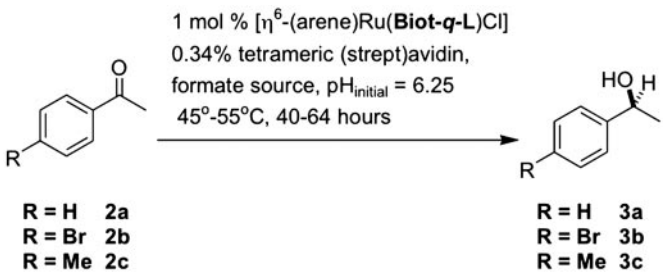

Scheme 3. Transfer hydrogenation of acetophenone derivatives **2 a-c** catalyzed by artificial metalloenzymes.

Table 1. Selected results for the chemical optimization of the performance of $[\eta^6$-(arene)Ru(Biot–*q*–L)Cl]⊂(strept)avidin as an artificial metalloenzyme for the transfer hydrogenation of acetophenone 2a

Entry	Ligand	η^6-arene	Protein	Conversion, %	ee, %
1*	**Biot–*p*–L**	*p*-cymene	WT-Sav	51	28 (*R*)
2†	**Biot–*p*–L**	*p*-cymene	WT-Sav	55	57 (*R*)
3†	**Biot–*p*–L**	*p*-cymene	WT-Avi	24	22 (*R*)
4†	**Biot–*m*–L**	*p*-cymene	WT-Sav	20	6 (*S*)
5†	**Biot–*o*–L**	*p*-cymene	WT-Sav	18	3 (*S*)
6†	**Biot–*p*–L**	Benzene	WT-Sav	29	56 (*S*)
7†	**Biot–*p*–L**	Benzene	WT-Avi	17	17 (*R*)

All catalytic runs were carried out at 45°C for 40 h at $pH_{initial}$ = 6.25, using a Ru/acetophenone **2a**/formate ratio of 1:100:4,200. Conversions and enantioselectivities were determined by HPLC on Chiralcel OB-H.
*Nonbuffered 0.5 M formate solution.
†Mixed buffer HCO_2Na (0.5 M) + $B(OH)_3$ (0.47 M).

(*iii*) With streptavidin as host protein, substitution of the η^6-(*p*-cymene)- by an η^6-benzene cap on the biotinylated piano-stool complex produces the opposite enantiomer of phenylethanol {57% (*R*), 55% conversion for $[\eta^6\text{-(}p\text{-cymene)Ru(}$**Biot–*p*–L**$\text{)Cl}]\subset$streptavidin and 56% ee (*S*), 29% conversion for $[\eta^6$-(benzene)Ru(**Biot–*p*–L**)Cl]⊂streptavidin, respectively; Table 1, entries 2 and 6}.

Having identified the best biotinylated ligand–η^6-arene combinations, we proceeded to genetically optimize the performance of the artificial metalloenzyme by introducing point mutations within the host protein. For this purpose, a recombinant avidin with a lowered isoelectric point (r-GAvi, pI = 5.4) (44) and five streptavidin mutants (S112G Sav, K80G Sav, V47G Sav, P64G Sav, and the double mutant P64G S112G Sav) (28) were screened. For the reduction of acetophenone using the boric acid·formate mixed buffer, some additional general trends emerge (Table 2):

(*i*) The host protein with the mutation closest to the catalytic site (S112G Sav) affords the highest conversions but the lowest selectivity {28% ee (*R*), 90% conversion using $[\eta^6\text{-(}p\text{-cymene)Ru(}$**Biot–*p*–L**$\text{)Cl}]\subset$S112G Sav; 8% ee (*S*), 42% conversion using $[\eta^6$-(benzene)Ru(**Biot–*p*–L**)Cl]⊂S112G Sav; Table 2, entries 2 and 7}.

(*ii*) The host protein with the most remote site of mutation (P64G Sav) has the greatest influence on the enantioselectivity

Table 2. Selected results for the genetic optimization of the performance of $[\eta^6$-(arene)Ru(Biot–*p*–L)Cl]⊂(strept)avidin as an artificial metalloenzyme for the transfer hydrogenation of acetophenone 2a by using formate·boric acid as a reducing agent

Entry	Ligand	η^6-arene	Protein	Conversion, %	ee, %
1	**Biot–*p*–L**	*p*-cymene	r-GAvi	40	22 (*R*)
2	**Biot–*p*–L**	*p*-cymene	S112G Sav	90	28 (*R*)
3	**Biot–*p*–L**	*p*-cymene	V47G Sav	42	68 (*R*)
4	**Biot–*p*–L**	*p*-cymene	K80G Sav	54	65 (*R*)
5	**Biot–*p*–L**	*p*-cymene	P64G Sav	54	72 (*R*)
6	**Biot–*p*–L**	*p*-cymene	P64G S112G Sav	95	58 (*R*)
7	**Biot–*p*–L**	Benzene	S112G Sav	42	8 (*S*)
8	**Biot–*p*–L**	Benzene	V47G Sav	8	56 (*S*)
9	**Biot–*p*–L**	Benzene	K80G Sav	31	51 (*S*)
10	**Biot–*p*–L**	Benzene	P64G Sav	30	58 (*S*)

All catalytic runs were carried out at 45°C for 40 h at $pH_{initial}$ = 6.25, using a Ru/acetophenone **2a**/formate ratio of 1:100:4,200, by using the mixed buffer HCO_2Na (0.5 M)+$B(OH)_3$ (0.47 M) as a formate source. Conversions and enantioselectivities were determined by HPLC on Chiralcel OB-H.

CHEMISTRY

Table 3. Selected results for the optimization of the performance of [η^6-(arene)Ru(Biot–*p*–L)Cl]⊂(strept)avidin as an artificial metalloenzyme for the transfer hydrogenation of acetophenone derivatives 2a-c by using formate·boric acid as a reducing agent in 0.15 M Mops buffer

Entry	Ligand	η^6-arene	Protein	Substrate	Temperature, °C	Time, h	Conversion, %	ee, %
1	**Biot–*p*–L**	*p*-cymene	Sav	**2a**	45	40	40	66 (*R*)
2	**Biot–*p*–L**	Benzene	Sav	**2a**	45	40	30	63 (*S*)
3	**Biot–*p*–L**	*p*-cymene	Sav	**2a**	55	64	82	68 (*R*)
4	**Biot–*p*–L**	*p*-cymene	P64G Sav	**2a**	55	64	90	85 (*R*)
5	**Biot–*p*–L**	*p*-cymene	P64G Sav	**2b**	55	64	97	89 (*R*)
6	**Biot–*p*–L**	*p*-cymene	P64G Sav	**2c**	55	64	92	94 (*R*)
7	**Biot–*p*–L**	*p*-cymene	P64G S112 G Sav	**2a**	55	40	Quantitative	67 (*R*)
8	**Biot–*p*–L**	*p*-cymene	P64G S112 G Sav	**2b**	55	40	Quantitative	88 (*R*)
9	**Biot–*p*–L**	*p*-cymene	P64G S112 G Sav	**2c**	55	40	Quantitative	90 (*R*)
10	**Biot–*p*–L**	Benzene	P64G Sav	**2c**	45	64	34	57 (*S*)
11	**Biot–*p*–L**	Benzene	P64G Sav	**2c**	55	64	44	44 (*S*)

All catalytic runs were carried out at $pH_{initial}$ = 6.25 by using the mixed buffer HCO_2Na (0.5 M) + $B(OH)_3$ (0.47 M) combined with Mops (0.15 M) with a Ru/substrate **2 a-c**/formate ratio of 1:100:4,500. Conversions and enantioselectivity were determined by HPLC on Chiralcel OB-H.

{72% ee (*R*), 54% conversion for [η^6-(*p*-cymene)Ru(**Biot–*p*–L**)Cl]⊂P64G Sav; 58% ee (*S*), 30% conversion with [η^6-(benzene)Ru(**Biot–*p*–L**)Cl]⊂P64G Sav; Table 2, entries 5 and 10}.

(*iii*) The double mutant P64G S112G Sav (Table 2, entry 6) combines the features of both single mutants P64G (increased selectivity vs. WT Sav) and increased activity S112G (increased activity vs. WT Sav).

With the aim of further stabilizing the pH ≈6.25, various buffers were screened. Addition of 0.15 M Mops [3-(*N*-morpholino)propanesulfonic acid sodium salt, pH_{final} <7.0] to the formate·boric acid mixture has a beneficial effect on the enantioselectivity, at the cost of a slightly lower conversion, however (compare Table 3, entries 1 and 2 with Table 1, entries 2 and 6). To overcome this drawback, the temperature was raised from 45°C to 55°C, and the reaction time was extended to 64 h (Table 3, entry 3). In the presence of Mops at 55°C, [η^6-(*p*-cymene)Ru(**Biot–*p*–L**)Cl]⊂P64G Sav affords (*R*)-phenylethanol in 85% ee (*R*) in 90% conversion (Table 3, entry 4, compare with Table 2, entry 5).

Next, *p*-bromoacetophenone **2b** and *p*-methylacetophenone **2c** were tested in conjunction with [η^6-(*p*-cymene)Ru(**Biot–*p*–L**)Cl]⊂P64G Sav and [η^6-(benzene)Ru(**Biot–*p*–L**)Cl]⊂P64G Sav. Again with these substrates, the *p*-cymene-capped and the benzene-capped catalysts afford the opposite enantiomers within the same host protein (Table 3, entries 4–6 and 10–11). For example, the reduction of *p*-methylacetophenone **2c** affords *p*-tolylethanol in 94% ee (*R*) with 92% conversion and in 44% (*S*) with 44% conversion by using [η^6-(*p*-cymene)Ru(**Biot–*p*–L**)Cl]⊂P64G Sav and [η^6-(benzene)Ru(**Biot–*p*–L**)Cl]⊂P64G Sav, respectively (Table 3, entries 6 and 11).

It is interesting to note that increasing the temperature has a beneficial effect on both the conversion and enantioselectivity for the *p*-cymene-capped catalyst; in contrast, it has a detrimental effect on enantioselectivity for the benzene-capped catalyst (Table 3, compare entries 10 and 11).

At 55°C, the double mutant [η^6-(*p*-cymene)Ru(**Biot–*p*–L**)Cl]⊂P64G S112G Sav produces quantitatively all three phenylethanol derivatives (**2 a-c**) within 40 h with selectivities intermediate between the WT Sav and P64G Sav (Table 3, entries 7–9).

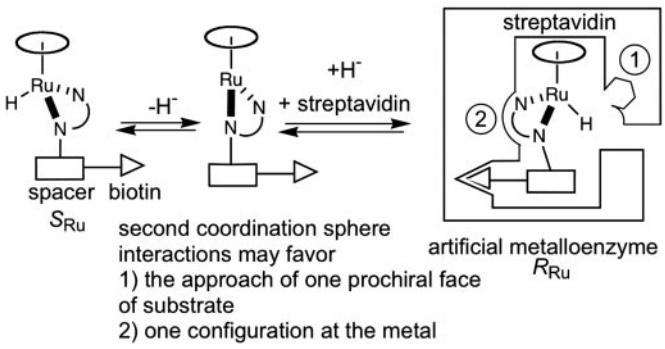

Scheme 4. Postulated second coordination sphere interactions between streptavidin and either [η^6-(arene)Ru(**Biot–*p*–L**)Cl] or the substrate. Depending on the η^6-arene cap, S_{Ru}⊂streptavidin or R_{Ru}⊂streptavidin may be favored.

Outlook

The study of artificial transfer hydrogenases based on biotin-avidin technology reveals several noteworthy features:

(*i*) Having identified a source of hydrogen compatible with streptavidin, biotinylated three-legged piano-stool complexes are versatile enantioselective transfer hydrogenation catalysts.

(*ii*) As the first coordination sphere around ruthenium is achiral, enantioselection is determined by second coordination sphere interactions. In this context, the choice of capping arene (either η^6-*p*-cymene or η^6-benzene) plays a critical role in determining which enantiomer of the product is produced preferentially. To rationalize this observation, two complementary enantioselection mechanisms can be envisaged. On one hand, protein–substrate interactions may favor the preferential approach of one prochiral face of the substrate. On the other hand, streptavidin–[η^6-(arene)Ru(**Biot–*q*–L**)Cl] contacts may enforce one configuration at ruthenium [(R_{Ru}) or (S_{Ru})] (45). This configuration, in turn, could determine which prochiral face of the substrate undergoes reduction. These two possibilities are summarized in Scheme 4.

(*iii*) Both chemical and genetic methodologies [i.e., chemogenetic (46)] can be efficiently combined to optimize the activity and selectivity of the artificial metalloenzymes [up to 94% ee (*R*) with 92% conversion with 1 mol% catalyst loading]. This approach thus adds another dimension to catalyst discovery and optimization.

In the spirit of enzymatic catalysis, providing a well defined second coordination sphere for a transition state that does not involve coordination of the substrate to the metal (see **1**, Fig. 1) is a promising approach. Additional efforts in this area should be centered on the microscopic reverse reaction: the kinetic resolution of secondary alcohols by Oppenauer oxidation.

We thank Belovo Egg Science and Technology (Bastogne, Belgium) for a generous gift of avidin and C. R. Cantor (Boston University, Boston)

for the streptavidin gene. This work was generously funded by Swiss National Science Foundation Grants FN 620-57866.99 and FN 200021-105192, National Research Programme 47 Supramolecular Functional Materials Grant FN 4047-057532, Chairmen of the European Research Councils' Chemistry Committees (CERC3) Grant FN 20C321-101071, and the Canton of Neuchâtel.

1. Jacobsen, E. N., Pfaltz, A. & Yamamoto, H., eds. (1999) *Comprehensive Asymmetric Catalysis* (Springer, Berlin), Vols. 1–3.
2. Noyori, R. & Hashiduchi, S. (1997) *Acc. Chem. Res.* **30,** 97–102.
3. Noyori, R. & Ohkuma, T. (2001) *Angew. Chem. Int. Ed.* **40,** 40–73.
4. Drauz, K. & Waldmann, H. (1995) *Enzyme Catalysis in Organic Synthesis: A Comprehensive Handbook* (VCH, Weinheim, Germany), Vols. 1–2.
5. Faber, K. (2004) *Biotransformations in Organic Chemistry* (Springer, Berlin), 5th Ed.
6. Stampfer, W., Kosjek, B., Moitzi, C., Kroutil, W. & Faber, K. (2003) *Angew. Chem. Int. Ed.* **41,** 1014–1017.
7. Nakamura, K., Yamanaka, R., Matsuda, T. & Harada, T. (2003) *Tetrahedron Asymmetry* **14,** 2659–2681.
8. Kroutil, W., Mang, H., Edegger, K. & Faber, K. (2004) *Curr. Opin. Chem. Biol.* **8,** 120–126.
9. Blaser, H.-U., Malan, C., Pugin, B., Spindler, F., Steiner, H. & Studer, M. (2003) *Adv. Synth. Catal.* **345,** 103–151.
10. Palmer, M. J. & Wills, M. (1999) *Tetrahedron Asymmetry* **10,** 2045–2061.
11. Yamakawa, M., Yamada, I. & Noyori, R. (2001) *Angew. Chem. Int. Ed.* **40,** 2818–2821.
12. Brandt, P., Roth, P. & Andersson, P. G. (2004) *J. Org. Chem.* **69,** 4885–4890.
13. Yamakawa, M., Ito, H. & Noyori, R. (2000) *J. Am. Chem. Soc.* **122,** 1466–1478.
14. Clapham, S. E., Hadzovic, A. & Morris, R. H. (2004) *Coord. Chem. Rev.* **248,** 2201–2237.
15. Pàmies, O. & Bäckvall, J.-E. (2003) *Chem. Rev.* **103,** 3247–3261.
16. Lo, H. C., Burriez, O., Kerr, J. B. & Fish, R. H. (1999) *Angew. Chem. Int. Ed.* **38,** 1429–1432.
17. Ruppert, R., Herrmann, S. & Steckhan, E. (1987) *Tetrahedron Lett.* **28,** 6583–6586.
18. Westerhausen, D., Herrmann, S., Hummel, W. & Steckhan, E. (1992) *Angew. Chem. Int. Ed.* **31,** 1529–1531.
19. Hollmann, F., Lin, P.-C., Witholt, B. & Schmid, A. (2003) *J. Am. Chem. Soc.* **125,** 8209–8217.
20. Gihani, M. T. E. & Williams, J. M. J. (1999) *Curr. Opin. Chem. Biol.* **3,** 11–15.
21. Tann, C.-M., Qi, D. & Distefano, M. D. (2001) *Curr. Opin. Chem. Biol.* **5,** 696–704.
22. Carey, J. R., Ma, S. K., Pfister, T. D., Garner, D. K., Kim, H. K., Abramite, J. A., Whang, Z., Guo, Z. & Lu, Y. (2004) *J. Am. Chem. Soc.* **126,** 10812–10813.
23. Reetz, M. T., Rentzsch, M., Pletsch, A. & Maywald, M. (2002) *Chimia* **56,** 721–723.
24. Ohashi, M., Koshiyama, T., Ueno, T., Yanase, M., Fujii, H. & Watanabe, Y. (2003) *Angew. Chem. Int. Ed.* **42,** 1005–1008.
25. Reetz, M. T. (2004) *Proc. Natl. Acad. Sci. USA* **101,** 5716–5722.
26. Wilson, M. E. & Whitesides, G. M. (1978) *J. Am. Chem. Soc.* **100,** 306–307.
27. Lin, C.-C., Lin, C.-W. & Chan, A. S. C. (1999) *Tetrahedron Asymmetry* **10,** 1887–1893.
28. Skander, M., Humbert, N., Collot, J., Gradinaru, J., Klein, G., Loosli, A., Sauser, J., Zocchi, A., Gilardoni, F. & Ward, T. R. (2004) *J. Am. Chem. Soc.* **126,** 14411–14418.
29. Collot, J., Humbert, N., Skander, M., Klein, G. & Ward, T. R. (2004) *J. Orgomet. Chem.* **689,** 4868–4871.
30. Collot, J., Gradinaru, J., Skander, M., Humbert, N., Zocchi, A. & Ward, T. R. (2003) *J. Am. Chem. Soc.* **125,** 9030–9031.
31. Kada, K., Kaiser, K., Falk, H. & Gruber, H. J. (1999) *Biochim. Biophys. Acta* **1427,** 44–48.
32. Akakabe, Y., Takahashi, M., Kamezawa, M., Kikuchi, K., Tachibana, H., Ohtani, T. & Naoshima, Y. (1995) *J. Chem. Soc. Perkin Trans.* **1,** 1295–1298.
33. Kitamura, M., Oka, H. & Noyori, R. (1999) *Tetrahedron* **55,** 3605–3614.
34. Ueno, T., Ohashi, M., Kono, M., Kondo, K., Suzuki, A., Yamane, T. & Watanabe, Y. (2004) *Inorg. Chem.* **43,** 2852–2858.
35. Bubert, C., Blacker, J., Brown, S. M., Crosby, J., Fizjohn, S., Muxworthy, J. P., Thorpe, T. & Williams, J. M. J. (2001) *Tetrahedron Lett.* **42,** 4037–4039.
36. Thorpe, T., Blacker, J., Brown, S. M., Bubert, C., Crosby, J., Fitzjohn, S., Muxworthy, J. P. & Williams, J. M. J. (2001) *Tetrahedron Lett.* **42,** 4041–4043.
37. Hayes, A., Clarkson, G. & Wills, M. (2004) *Tetrahedron Asymmetry* **15,** 2079–2084.
38. Ma, Y., Liu, H., Chen, L., Cui, X., Zhu, J. & Deng, J. (2003) *Org. Lett.* **5,** 2103–2106.
39. Rhyoo, H. Y., Park, H.-J. & Chung, Y. K. (2001) *Chem. Commun.* 2064–2065.
40. Wu, X., Li, X., Hems, W., King, F. & Xiao, J. (2004) *Org. Biomol. Chem.* **2,** 1818–1821.
41. Bayer, E. A., Ehrligh-Rogozinski, S. & Wilchek, M. (1996) *Electrophoresis* **17,** 1319–1324.
42. Humbert, N., Zocchi, A. & Ward, T. R. (2005) *Electrophoresis* **26,** 47–52.
43. Abura, T., Ogo, S., Watanabe, Y. & Fukuzumi, S. (2003) *J. Am. Chem. Soc.* **125,** 4149–4154.
44. Zocchi, A., Jobé, A. M., Neuhaus, J.-M. & Ward, T. R. (2003) *Protein Expression Purif.* **32,** 167–174.
45. Therrien, B. & Ward, T. R. (1999) *Angew. Chem. Int. Ed.* **38,** 405–408.
46. Qi, D., Tann, C.-M., Haring, D. & Distefano, M. D. (2001) *Chem. Rev.* **101,** 3081–3111.